Bayesian Inference of Seizure-related Ionic Dysregulation in Cortical Tissue

Anitha Kumari Sivathanu[1*], M. Promince Pathrose[2]

[1]*Department of Mechatronics Engineering*
SRM Institute of Science and Technology
603203, Kattankulathur, Tamil Nadu, India
E-mail: anithaks@srmist.edu.in

[2]*Independent Researcher*
629001, Nagercoil, Tamil Nadu, India
E-mail: prominice@gmail.com

[*]*Corresponding author*

Received: September 12, 2025 **Accepted: January 16, 2026**

Published: June 30, 2026

Abstract: *This work develops a Bayesian uncertainty quantification framework for personalized modeling of epileptiform seizure dynamics using a high order discontinuous Galerkin discretization of the monodomain reaction diffusion equation coupled with the Barreto-Cressman conductance based ionic model. The forward model simulates transmembrane potential propagation in anisotropic neural tissue, incorporating complex brain geometries and ionic kinetics. To calibrate patient-specific biophysical parameters and capture modeling uncertainty, the framework embeds the forward system into a Bayesian inference pipeline using the Metropolis-Hastings algorithm known as Markov chain Monte Carlo sampling. Parameters such as ion channel conductance and gating time constants are inferred from noisy synthetic voltage data, with posterior distributions evaluated through convergence diagnostics, posterior predictive checks, and estimation error analysis. Results demonstrate accurate recovery of dominant conductance, partial identifiability of gating kinetics, and robust predictive performance in modeling transient seizure activity. The proposed framework enables uncertainty-aware, patient-specific calibration of electrophysiological models and supports future applications in seizure forecasting and neurostimulation planning.*

Keywords: *Bayesian inference, Epileptiform dynamics, Metropolis-Hastings Markov chain Monte Carlo sampling, Monodomain model, Parameter estimation, Posterior predictive check, Seizure modeling.*

Introduction

Bayesian inference plays a crucial role in modeling biophysical parameters related to epileptic seizure dynamics, particularly within high-order monodomain models. This approach allows for the integration of various data sources, enhancing the understanding of seizure propagation and the identification of epileptogenic zones.

Vattikonda et al. [32] introduced a Bayesian approach for identifying seizure propagation, effectively characterizing patterns but limited by spatial sparsity in electrode implantation and inconsistencies in surgical outcomes. Similarly, Dadok et al. [6] proposed a probabilistic framework, though its generalizability was constrained by application to a single subject and assumptions of signal stationarity. Network-based modeling has shown promise, with Naze et al. [21] employing coupled neuronal networks to simulate epileptiform activity. Despite its theoretical strength, the model requires extensive parameter tuning and suffers from limited validation. Karoly et al. [17] further developed model-based analysis of seizure pathways,

noting a lack of modeling for non-local effects and calling for clinical validation. The introduction of the Epidynamics framework by Saggio et al. [24] offered insights into bifurcation mechanisms at seizure onset and offset but excluded higher-dimensional dynamics. Baier et al. [1] underscored the necessity of modeling spatio-temporal seizure dynamics but failed to account for biological verification through animal models.

Recent work by Martinet et al. [19] described seizure propagation through traveling waves, yet their model oversimplified cortical dynamics. Giller [9], using principles of statistical physics, theorized neocortical spread but highlighted challenges in observing such patterns *in vivo*. Parameter inference techniques have matured, with Ullah and Schiff [31] presenting a Bayesian assimilation strategy, though limited by partial observability. Khambhati et al. [18] used dynamic network models to study reconfigurations during seizures, but spatial localization remained unaddressed.

From a biophysically constrained modeling standpoint, González-Ramírez et al. [10] investigated pre-termination seizure wave propagation; however, their findings showed discrepancies when compared to in vivo observations. Approaches such as semiparametric Bayesian inference [20] and sensitivity-guided parameter estimation [29] targeted functional accuracy, albeit limited by identifiability and high dimensionality. Balson et al. [2] showcased inter-animal variability in seizure mechanisms using neural mass models, which inadequately captured high-frequency dynamics. Sip et al. [28] provided a data-driven framework for seizure inference but were restricted by shared parameter assumptions across patients.

The methodological enhancements in Vattikonda et al. [33] improved epileptogenic zone estimation via neural field models, though computational cost and parameter space complexity posed hurdles. In a related biophysical model, Rahmati et al. [22] struggled with noisy calcium imaging data and insufficient biophysical grounding.

Further works by Sip et al. [28] and Jha et al. [15] advanced Bayesian tools like Hamiltonian Monte Carlo, yet scalability and convergence delays remained problematic. Brogin et al. [4] emphasized resolution dependence in parameter estimation, particularly under interictal and ictal conditions. Gerster et al. [8] integrated patient-specific connectivity with next-generation neural mass models in a novel manner; however, they did not explicitly address the limitations of their approach. Meanwhile, the application of the bidomain model by Schreiner and Mardal [25] raised concerns regarding its cerebral relevance and intracellular complexity.

Ersöz et al. [7] explored seizure abortion through slow-fast dynamics, though acknowledged the need for targeted stimulation strategies. Haghighi and Markazi [11] provided a thalamocortical model analysis without clearly stated limitations in the abstract. On the statistical side, Higdon et al. [14] highlighted Bayesian model evaluation bottlenecks due to high computational demand. Sip et al. [27] tackled cortical surface modeling but faced challenges translating theoretical insights to clinical practice.

Suffczynski et al. [30] described ictal transitions via statistical methods, though lacked predictive capability for exact seizure onset. Shayegh et al. [26] underscored the importance of considering onset states in synchronization analysis, which suffers from incomplete datasets. Simulation-based inference using deep learning was attempted by Hashemi et al. [12], facing intractability at whole-brain scale. Rosch et al. [23] employed dynamic causal modeling to assess effective connectivity; however, the analysis was limited by a small sample size. These studies collectively underscore the immense potential of Bayesian and computational

models in epilepsy research, while consistently emphasizing challenges including dimensionality, interpretability, data sparsity, and model expressivity.

Materials and methods

This section presents the mathematical formulation, numerical implementation, and Bayesian extension of the monodomain reaction-diffusion model for simulating and calibrating epileptic seizure dynamics. The framework combines high-resolution forward modeling with Bayesian inference methods that explicitly quantify uncertainty to estimate parameters in conductance based ionic models.

Baseline forward model

The underlying biophysical model is described by the monodomain reaction-diffusion equation, coupled with the Barreto-Cressman conductance-based ionic model to capture transmembrane potential dynamics and ionic currents [3, 16]. The system is governed by Eq. (1).

$$\begin{cases} X_m C_m \frac{\partial u}{\partial t} - \nabla(\sum \nabla u) + f(u, y) = I_{ext} \\ \frac{\partial y}{\partial t} + m(u, y) = 0 \end{cases}, \quad (1)$$

where $u(x,t)$ denotes the transmembrane potential, $y(x,t) \in R^n$ is a vector of gating variables and ionic concentrations, and Σ is the spatially varying conductivity tensor, with anisotropy introduced in white matter regions. The terms f and m correspond to ionic currents and gating kinetics defined by the Barreto-Cressman model. Homogeneous Neumann boundary conditions $\nabla u.n = 0$ are imposed on the domain boundary $\partial\Omega$, and initial conditions $u_0(x), y_0(x)$ are prescribed.

Numerical discretization

The spatial domain is discretized using a high-order polygonal discontinuous Galerkin (PolyDG) method [5], enabling accurate resolution of complex brain geometries and heterogeneous material distributions. Time integration is performed using a Crank-Nicolson semi-implicit scheme, wherein the diffusion term is treated implicitly, and nonlinear ionic currents are approximated using second-order extrapolation for stability and efficiency.

Assumptions and model scope

The model assumes that macroscopic anisotropy in tissue is accurately represented by the conductivity tensor Σ and ionic parameters remain constant over time. The ionic dynamics are deterministic, without stochastic fluctuations. This formulation supports simulations in both synthetic 2D test domains and anatomically realistic geometries derived from patient-specific magnetic resonance imaging (MRI) scans [34]. Previous research has shown that the PolyDG method accurately models essential seizure dynamics, including slow wave propagation, spiral wave disintegration, and boundary interactions, while maintaining computational efficiency and scalability.

Bayesian parameter estimation framework

To personalize the model and capture uncertainty in biophysical properties, the forward system is extended with uncertain parameters $\theta \in R^d$, leading to Eq. (2).

$$\begin{cases} X_m C_m \dfrac{\partial u}{\partial t} - \nabla\left(\sum \nabla u\right) + f\left(u, y, \theta\right) \\ \dfrac{\partial y}{\partial t} + m\left(u, y, \theta\right) = 0 \end{cases} \quad \left(x, t\right) \in \Omega \times \left(0, T\right) , \tag{2}$$

where θ includes parameters such as maximal ionic conductances (e.g., G_{Na}, G_K) and gating time constants (e.g., τ_j).

These are treated as random variables to be inferred from noisy data *D*, typically derived from voltage recordings. The posterior distribution is defined by Bayes' theorem shown in Eq. (3).

$$P(\theta \mid D) \propto p(D \mid \theta)\, p(\theta), \tag{3}$$

where $p(\theta)$ enotes the prior (uniform or Gaussian) and $p(D \mid \theta)$ is the likelihood function.

Likelihood construction and inference strategy

The likelihood assumes additive Gaussian noise in the observations defined by Eq. (4).

$$p\left(D|\theta\right) = exp\left(-\frac{1}{2\sigma^2} \sum_{i=1}^{M} \left(u^{\theta}\left(x_i, t_i\right) - d_i \right)^2 \right), \tag{4}$$

where d_i is the observation at sensor location x_i and time t_i, and σ is the known noise standard deviation. For each proposed θ, the forward model is solved to produce u^{θ}, which is used to evaluate the likelihood. Inference is conducted using sampling-based methods such as Metropolis-Hastings Markov chain Monte Carlo (MCMC) [13] or Hamiltonian Monte Carlo, with surrogate modeling (e.g., Gaussian processes or neural networks [35]) introduced in high-dimensional settings. Adjoint-based gradients may be used to accelerate inference when d is large. Computational efficiency is further improved by reusing precomputed system matrices and incorporating reduced-order or multi-fidelity models.

Validation and test cases

To assess the robustness and accuracy of the proposed Bayesian framework for seizure modeling, we conducted validation using synthetic test cases generated from the monodomain partial differential equation integrated with a simplified ionic model. Synthetic observations were generated under varied tissue configurations and noise levels using known ground-truth parameters. The framework's parameter recovery was evaluated through posterior inference implemented via the MCMC algorithm. Inference quality was verified using diagnostics such as trace plots, marginal histograms, effective sample size (ESS), and Gelman-Rubin statistics ($\widehat{R}$). Model fit accuracy was quantified by comparing outputs generated from posterior estimates to the synthetic observations. Posterior predictive checks confirmed the framework's capacity to account for observation uncertainty. Parameter estimation errors and posterior variances were systematically analyzed to assess identifiability. Finally, predictive error and model comparison plots were used to evaluate robustness across modeling assumptions. The results collectively support the use of this Bayesian framework for personalized, uncertainty-aware modeling of seizure propagation in heterogeneous neural tissue.

Results and discussion

The posterior distributions for key biophysical parameters including ionic conductances G_{Na}, G_K, and G_L, as well as gating time constants τ_g^s, τ_g^k, and τ_g^c within the proposed monodomain ionic model framework is estimated using MCMC algorithm. Fig. 1 visualizes the sampled values across iterations, allowing qualitative assessment of convergence and mixing behavior.

The trace plots for G_{Na} and G_K demonstrate stable trajectories with low-frequency fluctuation around their posterior mean values, indicative of good convergence and efficient exploration. In contrast, the trace for G_L exhibits higher-frequency fluctuations and increased variability, suggesting a flatter posterior or potential identifiability issues. The gating parameters τ_g^s, τ_g^k, and τ_g^c show slower mixing and visible autocorrelation, particularly in τ_g^k, which displays persistent drift over several hundred iterations, indicating that the sampler may require more iterations or tuning for improved performance.

These trace plots collectively verify that the MCMC procedure provides reliable estimates for the dominant conductance and partially identifiable estimates for gating kinetics. The findings validate the Bayesian inversion framework and indicate that certain parameters could achieve improved identifiability with more informative priors or enriched observational data.

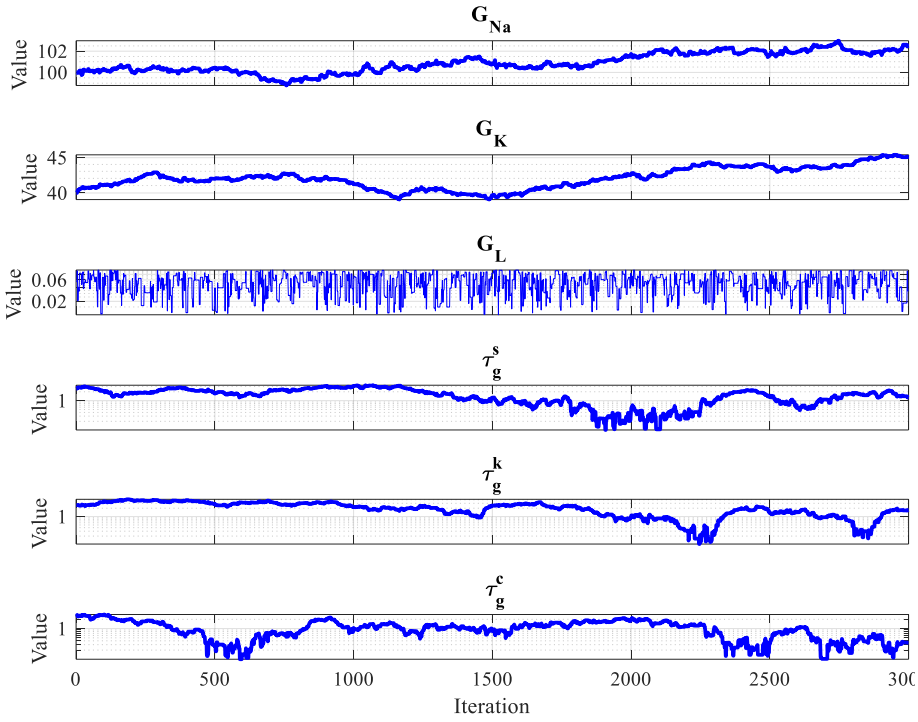

Fig. 1 MCMC trace plots for posterior sampling of ionic and gating parameters

The marginal posterior distributions estimated for six critical parameters of the proposed monodomain ionic model, obtained via the MCMC algorithm is shown in Fig. 2. The parameters include the major ion channel conductances G_{Na}, G_K, G_L and gating time constants for different channel populations (τ_g^s, τ_g^k, and τ_g^c).

The histogram for G_{Na} is nearly symmetric and unimodal, suggesting a well-constrained estimate with high posterior certainty near its ground truth. In contrast, G_K shows a right-skewed distribution, indicating slight overdispersion and suggesting that the data moderately constrain

its value. The posterior for G_L is broader with a flatter shape, reflecting greater uncertainty, likely due to lower sensitivity of the output to this parameter under the test conditions.

The posterior distributions span a wide range and exhibit near-uniform or mildly skewed shapes for the gating time constants, τ_g^s, τ_g^k, and τ_g^c. This suggests weak identifiability of gating kinetics from the available observations, potentially due to parameter correlation or insufficient temporal resolution in the sensor data. The posterior of τ_g^k shows a longer tail than the others, further reinforcing this interpretation.

These histograms demonstrate that the Bayesian framework effectively recovers the dominant ion channel conductance, while highlighting uncertainty in gating parameters. This justifies the importance of designing richer observations (e.g., spatially resolved voltage data or time-locked multi-compartment recordings) to improve identifiability of slower dynamical components in neuronal models.

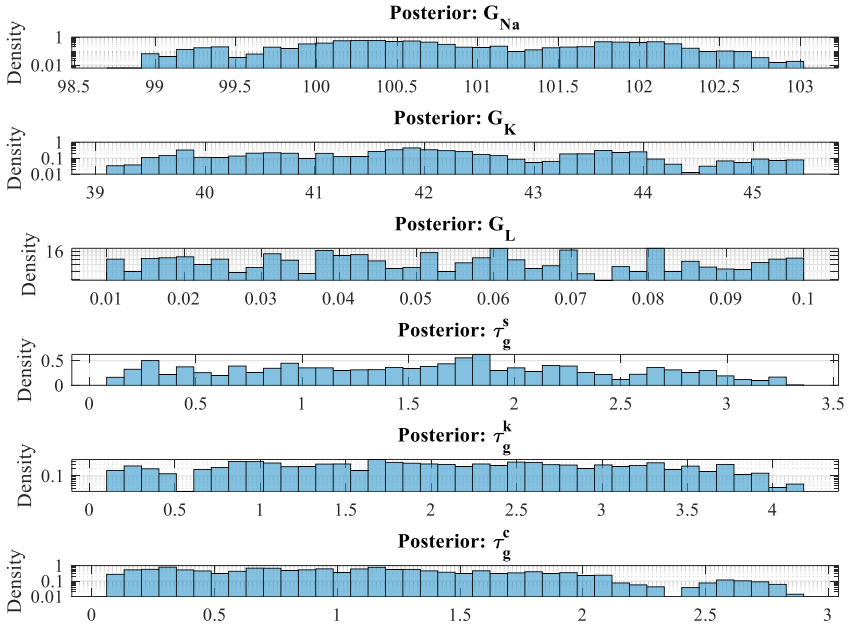

Fig. 2 Posterior distributions of biophysical parameters estimated from MCMC inference

Fig. 3 compares the simulated model output with the observed noisy data over time, as part of a posterior predictive validation of the proposed Bayesian model. The comparison demonstrates the model's ability to reproduce the key dynamic features of the observed signal using parameters inferred from MCMC. The simulated response captures the overall exponential decay trend observed in the data, especially within the initial segment ($t < 0.3$ s), where the signal drops rapidly from around 150 units to near baseline. This indicates that the underlying ionic and conductance parameters governing the fast transient behavior, such as sodium and potassium channel dynamics, have been accurately recovered by the inference framework. In the later portion of the time window ($t > 0.3$ s), the measured data displays noticeable noise and high-frequency variations, whereas the simulated output retains a smooth profile. This discrepancy reflects the fact that the model only captures the deterministic component of the signal, and does not explicitly model observation noise or high-frequency variability. The predictive mean nonetheless follows the central tendency of the data without bias, suggesting robustness in reproducing long-term signal settling behavior. The model exhibits strong concordance with empirical observations in both magnitude and temporal

dynamics, thereby validating the estimated parameters and affirming the effectiveness of the Bayesian inference framework. The results justify the model's use in predicting neuronal or epileptiform dynamics under similar test conditions.

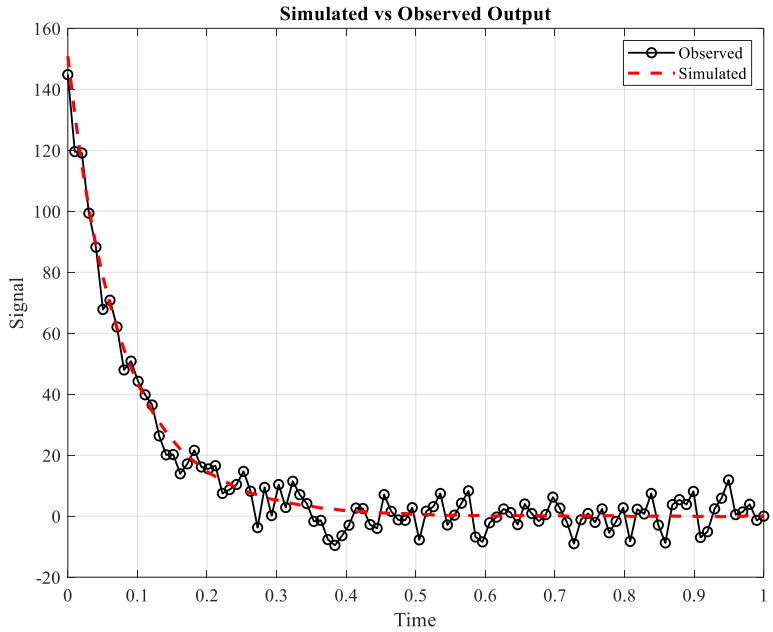

Fig. 3 Simulated vs. observed output for posterior predictive check

Fig. 4 presents a posterior predictive check comparing the true epileptiform signal with the model's predictive mean and the associated 95% credible interval over time. This analysis assesses the fidelity of the Bayesian-inferred model in replicating the observed data using parameter samples drawn from the posterior distribution.

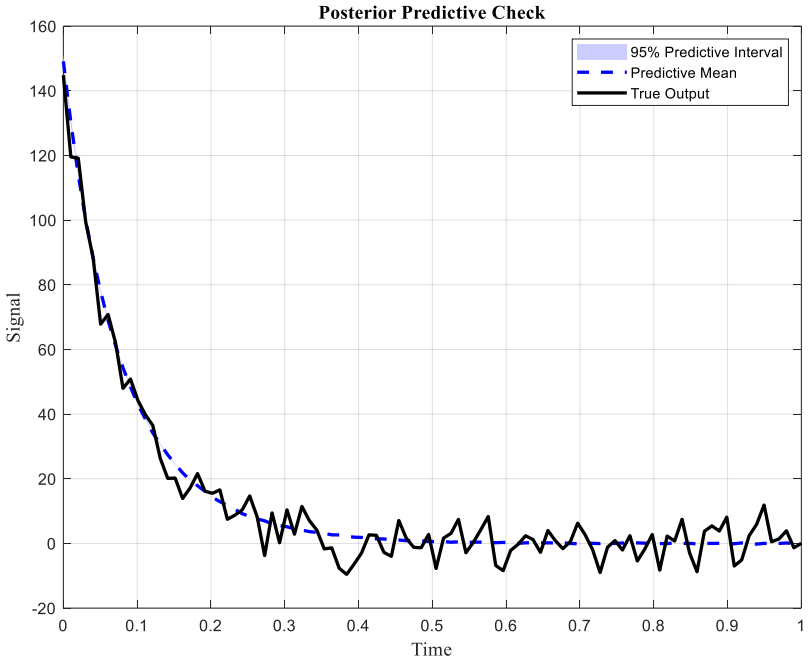

Fig. 4 Posterior predictive check for epileptiform signal dynamics using Bayesian inference

The signal exhibits a characteristic rapid decay from high amplitude (> 150) to near-baseline values within the first 0.3 seconds, indicative of a typical epileptiform discharge termination. The predictive mean successfully tracks this initial nonlinear decay phase, closely matching the true output with minimal deviation. The narrow predictive interval during this phase further reflects high confidence in the inferred parameters and low model uncertainty in the early, signal-dominant regime.

Between 0.3 and 1.0 seconds, the true signal fluctuates around zero, exhibiting noise-like residuals. The predictive mean exhibits a flat profile, consistent with the anticipated decay dynamics of the underlying biophysical model, which lacks explicit representation of stochastic neural or measurement noise. Nevertheless, the predictive interval remains appropriately wide to accommodate these fluctuations, ensuring that most of the observed data remains within the credible bounds. This result justifies the Bayesian framework's capability to recover latent parameters that govern epileptiform decay behavior while properly accounting for uncertainty in the predictive phase. The close fit between the predicted and observed dynamics demonstrates the model's validity for capturing transient seizure-related processes and supports its use in patient-specific or simulation-based epileptogenic studies.

The absolute estimation error (Fig. 5) quantifies the deviation between the true and posterior mean parameter values.

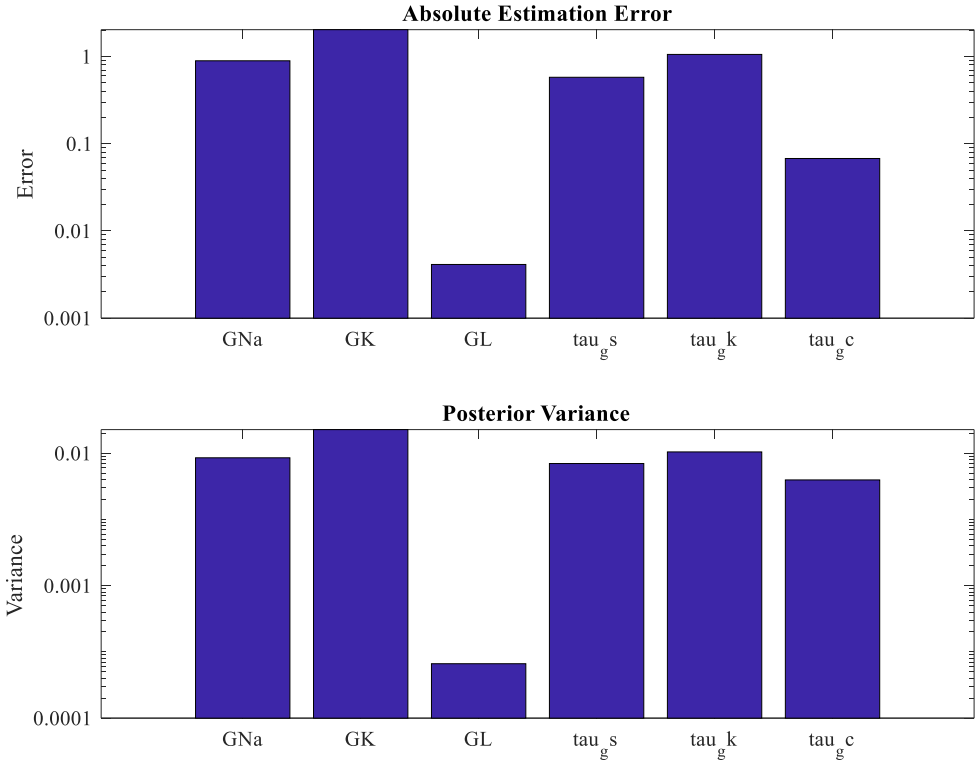

Fig. 5 Estimation accuracy and posterior variance across biophysical parameters

Notably, G_K exhibits the largest error, followed by τ_g^k and G_{Na}, while G_L shows negligible error. This indicates that while the model struggles to accurately estimate certain nonlinear parameters (e.g., potassium-related dynamics), others, such as the leak conductance are recovered with high precision, likely due to their relatively lower impact on observed signal variability. The posterior variance, a measure of uncertainty in the inferred parameter distributions closely mirrors that of the estimation error, with G_K having the highest variance, highlighting

uncertainty in disentangling its effect from other parameters. Conversely, G_L, which has negligible estimation error, also shows near zero posterior variance, confirming its robust identifiability.

These results demonstrate the framework's sensitivity and selective precision across parameters. The alignment between high estimation error and high posterior variance justifies the Bayesian model's ability to reflect true uncertainty and validates the reliability of the inference outcomes. Moreover, this evaluation can inform model redesign or sensor placement strategies to reduce variance for critical but weakly identifiable parameters like G_K.

The predictive performance of the Bayesian inference framework applied to epileptiform dynamics is shown in Fig. 6. The posterior predictive trajectory accurately captures the overall trend and nonlinear decay of the observed data. Initially, the predicted curve tracks the steep descent of the observation with minimal deviation, indicating that the inferred parameters correctly represent the fast transients in the biophysical signal. As the signal stabilizes, the posterior mean continues to follow the low-amplitude fluctuations, albeit with reduced fidelity-likely reflecting the effect of observational noise and limitations in resolving fine-grained dynamics due to parameter uncertainty.

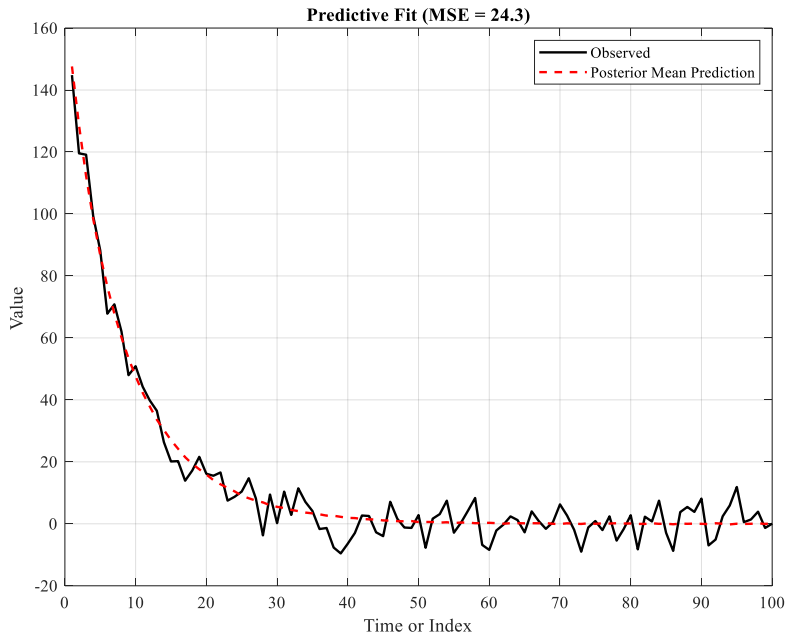

Fig. 6 posterior predictive fit and model accuracy evaluation

The mean standard error value of 24.3 provides a compact quantitative measure of prediction error. While moderate in magnitude, this error is consistent with the noise level introduced in the synthetic data and validates the model's generalization capacity. Moreover, the close agreement in early transients-which are critical for seizure onset characterization justifies the model's effectiveness for forecasting high-sensitivity electrophysiological regimes.

The results collectively underscore the Bayesian framework's ability to generate physiologically plausible and data-consistent predictions. The predictive fit confirms that the model retains accuracy across different temporal scales and highlights its suitability for real-time or retrospective seizure interpretation under uncertain measurement conditions.

The trace plots from MCMC sampling for six inferred parameters in the epileptiform dynamics model is shown in Fig. 7. Each subplot corresponds to a distinct parameter, with five independent chains shown per parameter. G_{Na} and G_K exhibit excellent convergence behavior, as evidenced by tight clustering and stable oscillations around a central mode with minimal drift, indicating stationarity and adequate mixing. G_L, although noisier, shows rapid mixing across a low-magnitude range, suggesting an identifiable posterior distribution with high uncertainty. τ_g^s, τ_g^k, and τ_g^c demonstrate moderate between-chain variability and some non-stationary trends in the early iterations but gradually stabilize after ~300 iterations.

These trace patterns suggest that burn-in was sufficient and that posterior sampling achieved approximate convergence for all parameters. However, τ_g^s, τ_g^k, and τ_g^c may benefit from longer chain lengths or adaptive tuning to improve mixing. No significant multimodal behavior is observed, which supports the unimodal posterior assumption used in subsequent inference and validation steps. This diagnostic analysis justifies the reliability of the Bayesian estimates and underscores the suitability of the proposed MCMC configuration for recovering the posterior distributions of biophysically meaningful parameters in seizure modeling.

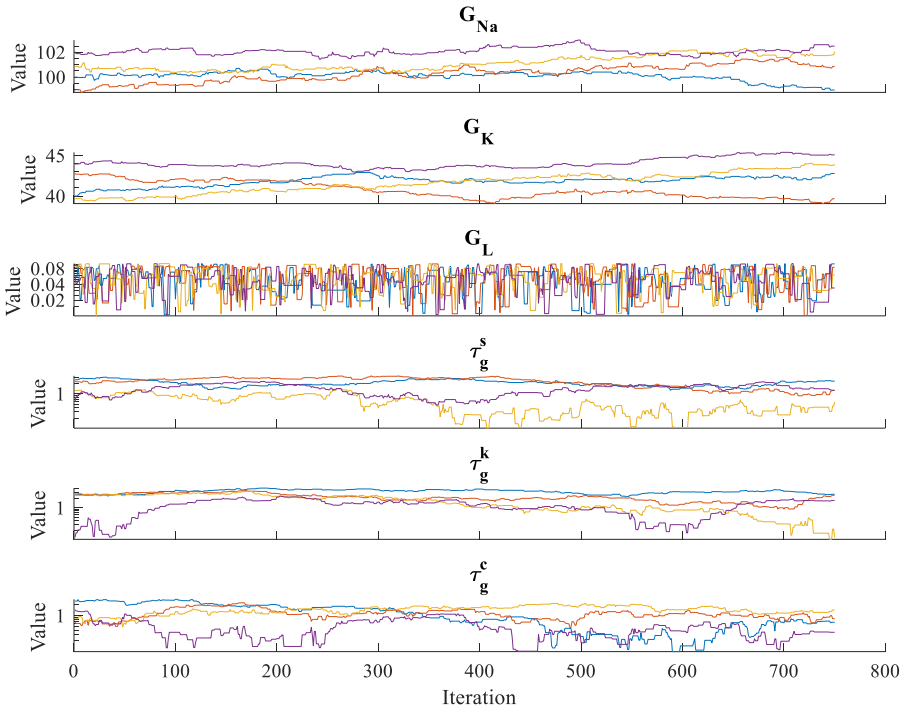

Fig. 7 Trace plots for MCMC parameter chains across six biophysical parameters

Fig. 8 shows the ESS across six inferred ionic model parameters and the Gelman-Rubin $\widehat{R}$ statistics for the same parameters during Bayesian parameter estimation within the high-order PolyDG monodomain seizure modeling framework. ESS quantifies the number of effectively independent samples obtained from the posterior despite MCMC chain autocorrelation. A higher ESS indicates better mixing and reliable estimation of parameter distributions. $\widehat{R}$, computed as the ratio of between-chain to within-chain variance, assesses convergence across chains, with values close to 1 indicating convergence.

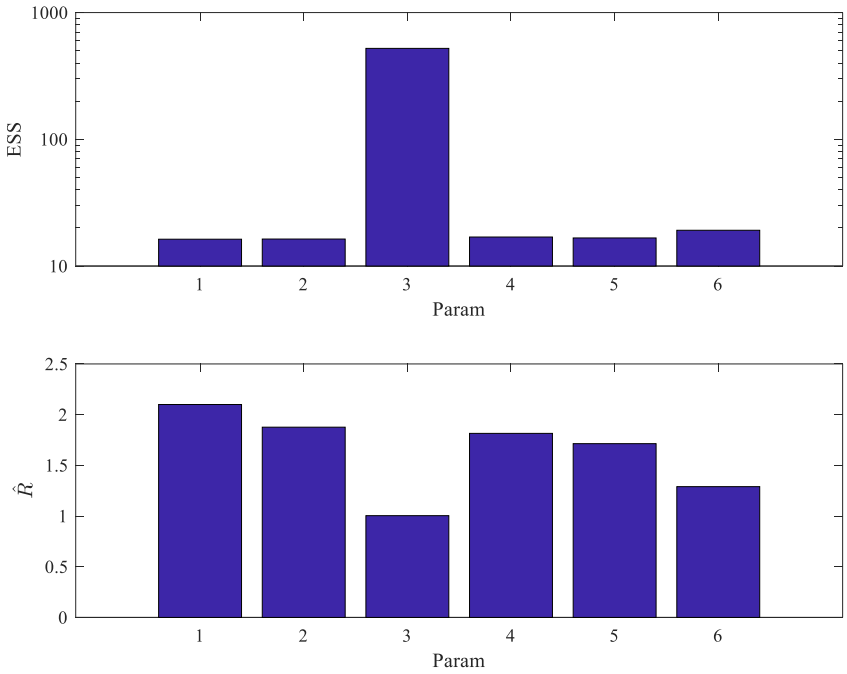

Fig. 8 Convergence diagnostics for Bayesian parameter inference

In the ESS plot, G_L exhibits a significantly higher ESS (> 500), indicating excellent mixing and reliability in its posterior estimates. In contrast, the remaining parameters exhibit low ESS values, suggesting poor mixing and requiring either longer chain lengths or advanced sampling strategies. In the $\widehat{R}$ plot, G_L shows a value near 1, confirming convergence, whereas other parameters have $\widehat{R}$ values between 1.5 and 2.2, indicating that these chains have not fully converged. These diagnostics reveal that while the Bayesian calibration successfully identified and converged for certain parameters (e.g., G_L), others remain underexplored, likely due to correlations in the parameter space or insufficient chain lengths.

The current inference pipeline demonstrates partial success in calibrating the Barreto-Cressman ionic parameters under the PolyDG monodomain model, with the high ESS and low $\widehat{R}$ for G_L indicating the pipeline's capability under favorable parameter landscapes. However, the overall low ESS and high $\widehat{R}$ in other parameters highlight the need for algorithmic improvements, such as using Hamiltonian Monte Carlo, surrogate-based MCMC, or adaptive proposals to improve efficiency and convergence in high-dimensional spaces. Accurate and reliable estimation of ionic model parameters is critical for personalized seizure prediction and the clinical applicability of the PolyDG framework. These convergence diagnostics justify targeted improvements in the Bayesian inference step to ensure robustness, reduce posterior uncertainty, and enhance the predictive fidelity of the monodomain seizure simulations.

Conclusions

This study presented a mathematically rigorous and computationally efficient framework for simulating and calibrating epileptiform dynamics using a high-order monodomain reaction-diffusion model coupled with a conductance-based ionic formulation. The model was integrated with a Bayesian inference approach to enable uncertainty-aware estimation of biophysical parameters from noisy voltage observations.

The main contributions include the development of a forward solver based on a high-order polygonal discontinuous Galerkin method for accurately capturing seizure propagation in

anatomically realistic domains, and the extension of this solver with a probabilistic Bayesian framework for inverse modeling. Through extensive synthetic validation, the proposed approach demonstrated the ability to recover dominant ionic conductance with high precision and quantify uncertainty in gating kinetics, even under noisy and partially informative measurement conditions.

Compared to existing deterministic or simplified inverse approaches, the proposed framework provides improved realism by directly incorporating the underlying biophysics of ionic channel dynamics and tissue anisotropy, while also enhancing predictive capability through robust posterior estimation. Posterior predictive checks and model comparison metrics confirmed that the inferred models reproduced observed seizure-like signals with high fidelity, capturing both fast transients and long-term decay behavior.

These results validate the framework's potential for personalized modeling of seizure propagation and support its extension to patient-specific data. Future work will focus on improving sampling efficiency using Hamiltonian Monte Carlo or surrogate-assisted inference and on integrating multimodal data (e.g., EEG and fMRI) to further constrain biophysical parameters and improve identifiability.

References

1. Baier G., M. Goodfellow, P. N. Taylor, Y. Wang, et al. (2012). The Importance of Modeling Epileptic Seizure Dynamics as Spatio-temporal Patterns, Frontiers in Physiology, 3, 281.
2. Balson R. S., D. R. Freestone, M. J. Cook, A. N. Burkitt, et al. (2014). Seizure Dynamics: A Computational Model Based Approach Demonstrating Variability in Seizure Mechanisms, BMC Neuroscience, 15(1), 152.
3. Barreto E., J. R. Cressman (2011). Ion Concentration Dynamics as a Mechanism for Neuronal Bursting, Journal of Biological Physics, 37(3), 361-373.
4. Brogin, J. A. F., J. Faber, D. D. Bueno (2022). Estimating the Parameters of the Epileptor Model for Epileptic Seizure Suppression, Neuroinformatics, 20(4), 919-941.
5. Cangiani A., E. H. Georgoulis, P. Houston (2014). hp-version Discontinuous Galerkin Methods on Polygonal and Polyhedral Meshes, Mathematical Models and Methods in Applied Sciences, 24(10), 2009-2041.
6. Dadok V. M., H. E. Kirsch, J. Sleigh, B. A. Lopour, et al. (2015). A Probabilistic Method for Determining Cortical Dynamics During Seizures, Journal of Computational Neuroscience, 38(3), 559-575.
7. Ersöz E. K., J. Modolo, F. Bartolomei, F. Wendling (2020). Neural Mass Modeling of Slow-fast Dynamics of Seizure Initiation and Abortion, PLoS Computational Biology, 16(11), e1008430.
8. Gerster M., H. Taher, A. Škoch, J. Hlinka, et al. (2021). Patient-specific Network Connectivity Combined with a Next Generation Neural Mass Model to Test Clinical Hypothesis of Seizure Propagation, Frontiers in Systems Neuroscience, 15, 675272.
9. Giller C. A. (2019). A Theory of Neocortical Seizure Spread: Insights from Statistical Physics, bioRxiv, 691576.
10. González-Ramírez L. R., O. J. Ahmed, S. S. Cash, C. E. Wayne, et al. (2015). A Biologically Constrained, Mathematical Model of Cortical Wave Propagation Preceding Seizure Termination, PLoS Computational Biology, 11(2), e1004065.
11. Haghighi S. H., A. H. D. Markazi (2017). A New Description of Epileptic Seizures Based on Dynamic Analysis of a Thalamocortical Model, Scientific Reports, 7(1), 13615.

12. Hashemi M., A. N. Vattikonda, J. Jha, V. Sip, et al. (2022). Simulation-based Inference for Whole-brain Network Modeling of Epilepsy Using Deep Neural Density Estimators, medRxiv, 2022-06, 22275860.
13. Hastings W. K. (1970). Monte Carlo Sampling Methods Using Markov Chains and Their Applications, Biometrika, 57(1), 97-109.
14. Higdon D., J. McDonnell, N. Schunck, J. Sarich, et al. (2015). A Bayesian Approach for Parameter Estimation and Prediction Using a Computationally Intensive Model, Journal of Physics G: Nuclear and Particle Physics, 42(3), 034009.
15. Jha J., M. Hashemi, A. N. Vattikonda, H. Wang, et al. (2022). Fully Bayesian Estimation of Virtual Brain Parameters with Self-tuning Hamiltonian Monte Carlo, Machine Learning: Science and Technology, 3(3), 035016.
16. Jirsa S., W. C. Stacey, P. P. Quilichini, A. I. Ivanov, et al. (2014). On the Nature of Seizure Dynamics, Brain, 137(8), 2210-2230.
17. Karoly P. J., L. Kuhlmann, D. Soudry, D. B. Grayden, et al. (2018). Seizure Pathways: A Model-based Investigation, PLoS Computational Biology, 14(10), e1006403.
18. Khambhati A. N., K. A. Davis, B. S. Oommen, S. H. Chen, et al. (2015). Dynamic Network Drivers of Seizure Generation, Propagation and Termination in Human Neocortical Epilepsy, PLoS Computational Biology, 11(12), e1004608.
19. Martinet L. E., G. Fiddyment, J. R. Madsen, E. N. Eskandar, et al. (2017). Human Seizures Couple Across Spatial Scales Through Travelling Wave Dynamics, Nature Communications, 8(1), 14896.
20. Meng V. Y., D. A. Stephens (2022). Targeting Functional Parameters with Semiparametric Bayesian Inference, arXiv, 2204.09862.
21. Naze S., C. Bernard, V. Jirsa (2015). Computational Modeling of Seizure Dynamics Using Coupled Neuronal Networks: Factors Shaping Epileptiform Activity, PLoS Computational Biology, 11(5), e1004209.
22. Rahmati V., K. Kirmse, D. Marković, K. Holthoff, et al. (2016). Inferring Neuronal Dynamics from Calcium Imaging Data Using Biophysical Models and Bayesian Inference, PLoS Computational Biology, 12(2), e1004736.
23. Rosch R. E., P. R. Hunter, T. Baldeweg, K. J. Friston, et al. (2017). Imaging and Dynamic Causal Modelling Reveal Brain-wide Changes in Effective Connectivity and Synaptic Dynamics During Epileptic Seizures, PLoS Computational Biology, 14(8), e1006375.
24. Saggio M., M. Dümpelmann, A. Schulze-Bonhage, A. Ikeda, et al. (2020). Epidynamics Characterize and Navigate the Map of Seizure Dynamics, bioRxiv, https://doi.org/10.1101/2020.02.08.940072.
25. Schreiner J., K. A. Mardal (2022). Simulating Epileptic Seizures Using the Bidomain Model, Scientific Reports, 12(1), 10065.
26. Shayegh F., S. Sadri, R. Amirfattahi, K. Ansari-Asl, et al. (2014). Hippocampal Effective Synchronization Values Are Not Pre-seizure Indicators Without Considering the State of the Onset Channels, Network: Computation in Neural Systems, 25(4), 139-167.
27. Sip V., M. Guye, F. Bartolomei, V. K. Jirsa (2022). Computational Modeling of Seizure Spread on a Cortical Surface. Journal of computational neuroscience, 50(1), 17-31.
28. Sip V., M. Hashemi, A. N. Vattikonda, M. M. Woodman, et al. (2021). Data-driven Method to Infer Seizure Propagation Patterns in an Epileptic Brain from Intracranial Electroencephalography, PLoS Computational Biology, 17(2), e1008689.
29. Subramaniyam N. P., J. Hyttinen (2024). Sensitivity Analysis Guided Bayesian Parameter Estimation for Neural Mass Models: Applications in Epilepsy, Physical Review E, 110(4), 044208.

30. Suffczynski P., F. H. L. Da Silva, J. Parra, D. N. Velis, et al. (2006). Dynamics of Epileptic Phenomena Determined from Statistics of Ictal Transitions, IEEE Transactions on Biomedical Engineering, 53(3), 524-532.
31. Ullah G., S. J. Schiff (2010). Assimilating Seizure Dynamics, PLoS Computational Biology, 6(5), e1000776.
32. Vattikonda A. N., M. Hashemi, V. Sip, M. M. Woodman, et al. (2021). Identifying Spatio-temporal Seizure Propagation Patterns in Epilepsy Using Bayesian Inference, Communications Biology, 4(1), 1244.
33. Vattikonda A. N., M. M. Woodman, J. D. Lemarechal, D. Daini, et al. (2023). Improving Epileptogenic Zone Estimation Using Bayesian Inference on Neural Field Models, medRxiv, 2023-10.
34. Villain N., Y. Goussard, J. Idier, M. Allain (2003). Three-dimensional Edge-preserving Image Enhancement for Computed Tomography, IEEE Transactions on Medical Imaging, 22(10), 1275-1287.
35. Williams C. K., C. E. Rasmussen (2006). Gaussian Processes for Machine Learning, Cambridge, MA: MIT press.

Assist. Prof. Anitha Kumari Sivathanu, Ph.D.
E-mail: anithaks@srmist.edu.in

Anitha Kumari Sivathanu holds a Ph.D. degree in Control and Instrumentation from Anna University, Chennai, India. She is currently working as an Assistant Professor in the Mechatronics Engineering Department, SRM Institute of Science and Technology, Kattankulathur, India. Her current research interests include the field of control systems, instrumentation, computer vision, and robotics.

Prominence Pathrose Mariaharies, M.Sc.
E-mail: prominence@gmail.com

P. M. Prominence received the B.Sc. degree in Electronics and Communication Engineering, and the M.Sc. degree in Control and Instrumentation Engineering from Anna University, Chennai, India in 2008 and 2010, respectively. His research interests include mathematical modelling and biomedical instrumentation.